Prague's Emission Fourier Transform Microwave Spectrometer – Design and Preliminary Results

Václav KABOUREK[1], Petr ČERNÝ[1], Petr PIKSA[1], Tomáš STUDECKÝ[2], Patrik KANIA[2], Štěpán URBAN[2]

[1] Dept. of Electromagnetic Field, Czech Technical University in Prague, Technická 2, 166 27 Prague, Czech Republic
[2] Dept. of Analytical Chemistry, Institute of Chemical Technology Prague, Technická 5, 166 28 Prague, Czech Republic

kabouvac@fel.cvut.cz, petr.cerny@fel.cvut.cz, stepan.urban@vscht.cz

Abstract. *The design, performance and operation of the spectrometer is based on the Fabry-Perot resonator supplemented by a pulsed supersonic nozzle for adiabatic cooling of the sample. The spectrometer's high sensitivity and resolution are demonstrated by several examples.*

Keywords

Fourier transform microwave spectrometer, rotational emission spectra, Fabry-Perot resonator, supersonic expansion, high resolution, sensitivity, hyperfine structure, molecular structure.

1. Introduction

Rotational microwave spectroscopy is a highly effective tool for the qualitative and quantitative analysis of gaseous samples [1], [2]. Although molecular rotation spectra are traditionally associated with molecular structure determination, today's microwave spectroscopy is connected with a wide variety of basic and applied problems in physical chemistry and molecular physics (such as molecular structure, conformational and tautomeric conversion, chemical bonding, charge transfer, internal dynamics, van der Waals complexes, astrophysical research, chemical analysis of atmosphere, etc.) [3].

All above-mentioned tasks are solved by analyzing the rotational structures of spectra, yet also through the analysis of their fine and hyperfine structures. It is possible to study fine and hyperfine molecular interactions successfully only through high resolution spectroscopy. Although high resolution symbolizes the obvious attribute of microwave spectroscopy, the measurement has to be performed at low pressures of the studied gas (approximately below 10 μbar), where pressure (collision) broadening and thus the possible overlap of spectral lines, are reduced to a minimum. Under these conditions, the widths of spectral lines are limited only by Doppler broadening ${}^{D}\Delta_{1/2}$

$$ {}^{D}\Delta_{1/2} = 7.16235 \cdot 10^{-7} \nu_0 \sqrt{T/M} \qquad (1) $$

where the parameter ${}^{D}\Delta_{1/2}$ represents the full width at half the maximum of a spectral line (FWHM), ν_0 is the frequency position of the spectral line, T stands for the temperature (K) and M symbolizes the molecular weight (amu). The relationship shows that the higher the molecular weight (and the lower the frequency) the narrower the spectral line. In microwave frequencies, the Doppler broadening ${}^{D}\Delta_{1/2}$ is typically within the kilohertz range (for example 12 kHz for a line at 10 GHz, 100 K and for a molecular weight of 100 amu).

Top quality measurements with very high spectral resolution require an extremely low sample pressure. On the other hand, it has a marked effect on the relaxation processes. In the lack of collisions (i.e. at low pressure), the relaxations of the excited rotational states are provided almost exclusively by spontaneous emission, which, according to the Planck's law, decreases with the third power of transition frequencies. Therefore, the relaxations of excited energy states are very slow (in comparison to e.g. the infra-red region). The populations of excited states are increasing and do not correspond to the thermodynamic equilibrium given by the Stefan-Boltzmann law (the lower energy level shows a higher population and vice versa). The probabilities of the induced emission and absorption are equal. The studied microwave transitions can become gradually saturated and the absorption spectrum is practically non-measurable. In other words, the standard microwave absorption spectroscopy of samples with negligible collision broadening becomes more difficult at low frequencies (i.e. below about 50 GHz) and falls behind emission microwave spectroscopy.

Due to the slow relaxation processes of the excited states at low microwave frequencies, as explained in the previous paragraph, the studied sample can be excited by a short microwave pulse. In addition, the subsequently emitted radiation can be down-converted and detected. The resulting decaying signal is transformed into the frequency domain with the help of the Fourier transformation. To date, the Fourier Transform Microwave (FTMW) emission spectroscopy with heterodyne detection is the most commonly used spectroscopic technique at frequencies below 30 GHz. Modern emission rotational spectroscopy was

developed around 1979 by Balle and Flygare, [4], [5]. In this type of FTMW spectrometer, the Fabry-Perot (FP) resonator, filled with the studied gas, is excited by a microwave impulse. The molecules are polarized by this excitation pulse. Consequently, the emitted signal is radiated at the same polarization direction and stored in a mode to which the resonator is tuned. The respective signal is coupled by feeding probes/antennas, then amplified and down-converted. The transient response of the excitation signal is recorded for the purpose of digital post-processing. The extension of the FTMW by a pulse nozzle enables the supersonic expansion of the sample into the vacuum chamber and a subsequent adiabatic cooling [6], which, in general, provides a significant sensitivity advantage for transitions originating from low-energy rotational levels in the vibrational ground state. FTMW spectroscopy is also a narrow-band technique due to the high quality factor of the FP resonator. The accuracy of the frequency position of the spectral lines can be enhanced by means of the atomic clock (e.g. a rubidium oscillator), synchronized by the long term standard, such as a Global Positioning System (GPS) time signal etc.

The principles of this FTMW spectrometer were inspired by the spectrometer designed by Flygare and Balle [4], [5] and developed by Grabow, [7]. To date, the aforementioned design provides the best performance in terms of the frequency resolution and intensity sensitivity. This paper discusses our specific construction, implementation and substantially extends the preliminary results published previously, [8], [9]. The paper is divided into the following sections. First, the specific design of the Fabry-Perot resonator is discussed. Second, the specific implementation of the experimental set-up is introduced. Finally, the preliminary experimental results are presented.

2. Fabry-Perot Resonator

The FP resonator serves as one of the key components of the FTMW spectrometer with heterodyne detection. Its parameters are predominantly determined by the parameters of the FP resonator, which commonly consists of two spherical mirrors. The sensitivity of the FTMW spectrometer to molecular signals increases with the resonator quality factor, which should exceed 10^4. The resonator dimensions determine substantially the lowest working frequency f_l of the spectrometer. The highest working frequency f_h is given by diffraction losses caused mainly by the roughness of resonator mirrors. In the FTMW spectrometer application, the frequency f_h is mainly limited by the operational bandwidth of the used electronics (approx. 26 GHz), see the next section.

Beside the intensity sensitivity, the widest frequency bandwidth is crucial for the spectroscopic application. Due to diffraction losses, the frequency f_l is given primarily by the FP resonator dimensions. The mirrors diameter D increases with the decreasing frequency f_l. The financial costs of the vacuum tank and diffusion pump are another very important limiting factor that hinders attainment of the lowest working frequency. Larger mirrors require a larger volume of the vacuum tank and thus a more efficient vacuum pump is needed in order to reach the best vacuum. As a result, it is necessary to find a compromise between the price and the widest frequency bandwidth available.

The diffraction losses for the dominant mode TEM_{00} of the FP resonator are negligible for the Fresnel number N higher than one. The Fresnel number N is defined by the equation

$$N = \frac{D^2}{4\lambda d} \tag{2}$$

where d is the mirrors distance, D is the mirror diameter, and λ stands for the wavelength. The higher modes of resonator are less suppressed when the Fresnel number is higher. Thus, the resonator dimensions are mainly designed for a low working frequency, where the Fresnel number equals one, see Fig. 1.

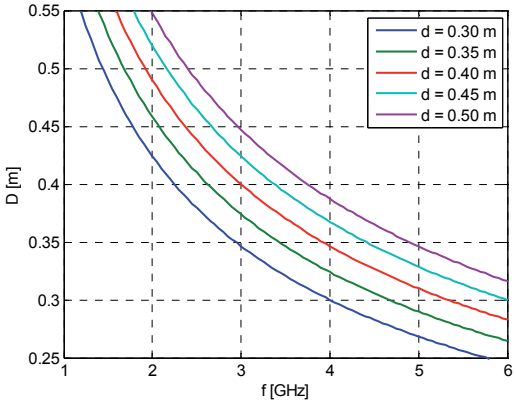

Fig. 1. The frequency dependence of mirror diameter D for Fresnel number $N = 1$ and different mirror distance d.

In order to make a reasonable compromise between the price and resonator parameters, we selected the frequency f_l equaling 3 GHz, the mirror diameter equal to 0.4 m and the middle mirror distance of 0.4 m. Indeed, the resonator should be stable. Its stability is defined by the non-equality

$$0 < g_1 g_2 < 1, \tag{3}$$

where $g_1 = 1 - d/R_1$, $g_2 = 1 - d/R_2$ and R_1 and R_2 are radii of the spherical mirrors curvature. The mirrors distance should differ from the confocal arrangement of mirrors ($g = 0$). The diffraction losses α_D, describing the ratio of resonator energy that is radiated out of the resonator, can be described by the approximation (4) [10], [11]

$$\alpha_D = 29 \cdot 10^{-4.83 \cdot N \cdot \sqrt{\frac{d}{R}}}. \tag{4}$$

The resonator diffraction quality factor (high values) is expressed by the approximation (5), see Fig. 2

$$Q_D = \frac{2\pi d}{\lambda \alpha_D}. \tag{5}$$

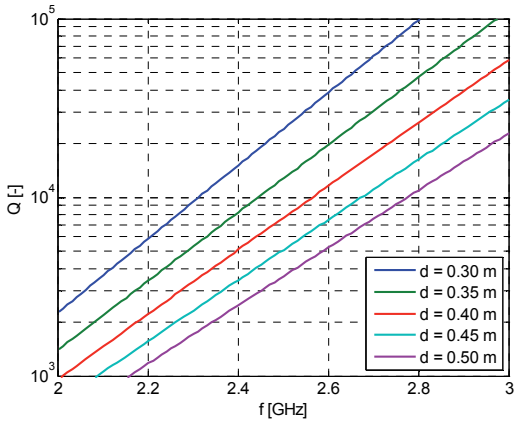

Fig. 2. The approximation of resonator diffraction quality factor (high values).

The quality factor reaches the value of 10^4 for the middle mirrors distance of 0.4 m and the frequency of approx. 2.56 GHz. The resonance condition for the general mode TEM_{plq} is defined as follows

$$\frac{2d}{\lambda} = q + (2p + l + 1)\frac{1}{\pi}\arccos\left(\sqrt{\left(1-\frac{d}{R_1}\right)\left(1-\frac{d}{R_2}\right)}\right) \quad (6)$$

where p and l define the type of mode TEM_{pl} and q states the number of half wavelengths inside the resonator. The resonator works optimally when the Fresnel number is larger than one, at the same time, is as close to one as possible, see the areas in Fig. 3 where the labels *"q = xx"* are located. In addition, the higher modes TEM_{pl} should not overlay the dominant mode TEM_{00}.

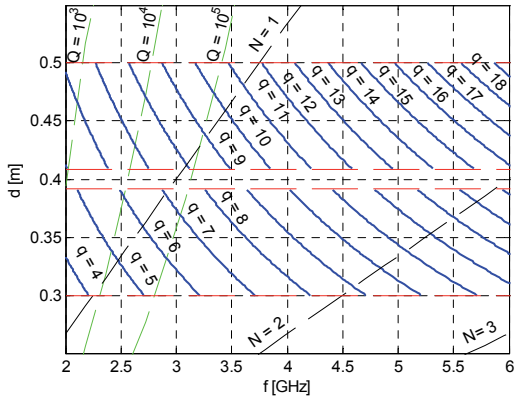

Fig. 3. Recommended tuning of FP resonator.

The beam radius w at the mirror is defined by the equation

$$w = \sqrt{\frac{\lambda R}{\pi\sqrt{2\frac{R}{d}-1}}}. \quad (7)$$

In the case of the FP resonator's shortest working wavelength, the feeding/coupling probes should be located inside the aforementioned beam width w. The entire operational frequency band (approx. 3–26 GHz) of the spectrometer is too wide for a single feeding. Thus it is divided into two sub-bands, which are consequently fed by two pairs of antennas. L-shaped wire hook antennas are designed for these sub-bands. In the case of wideband operation, their lengths are equal to $\lambda_{max}/4$, where λ_{max} represents the maximal wavelength (and minimal frequency, respectively) of the particular sub-band. In order to reach the highest possible sensitivity, the spectra are measured in narrow frequency bands and the antenna length should be adjusted to the operating wavelength $\lambda/4$. The antenna parameters are significantly influenced by the FP resonator coupling, tuning and quality factor. The transmitting or receiving antennas are mutually orthogonally oriented in order to reduce the leakage of the signal into the temporarily unused circuit of the system and, accordingly, to prevent the gaseous sample from being affected by the signal from the unused circuit.

The final design of the FP resonator comprises two spherical mirrors manufactured from the aluminum alloy (94.8 % Al, 4.5 % Mg, and 0.7 % Mn), with the diameter D = 0.4 m and the same radii for the spherical mirror curvature $R_{1,2}$ = 0.4 m. The distance between the mirrors d ranges from 0.32 to 0.48 m. In the case of the fixed mirror, the adjacent separation of the feeding pairs is 70 mm or 100 mm for both sub-bands respectively. The pulse valve is located in the centre of the mirror. This mirror is fixed, while the other one is movable. The arrangement of the feeding probes, pulse valve, and amplifiers is depicted in Fig. 4.

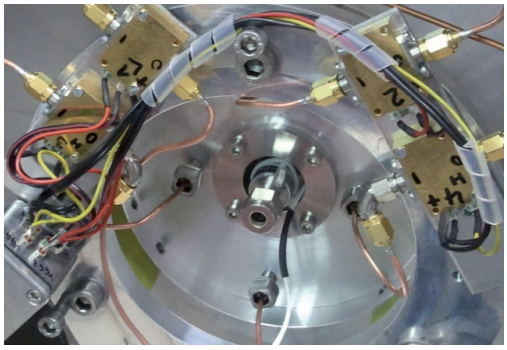

Fig. 4. The feeding probes and pulse valve arrangement in the case of the fixed mirror.

3. Fourier Transform Microwave Spectrometer

In this section, the overall FTMW spectrometer system is described, with the exception of the FP resonator that was described in detail above. The vacuum pump evacuates the resonator between the particular measurement cycles (i.e. between each gas injection). The amount of gas that has to be evacuated is determined by the length and repetition frequency of the excitation pulse, the diameter of the supersonic jet and the volume of the resonator. In this case, the DIP 8000 diffusion pump and TRIVAC D 65 B oil-sealed rotary vane pump at a rate (speed) of 8,000 l/s ensure that the pressure in the

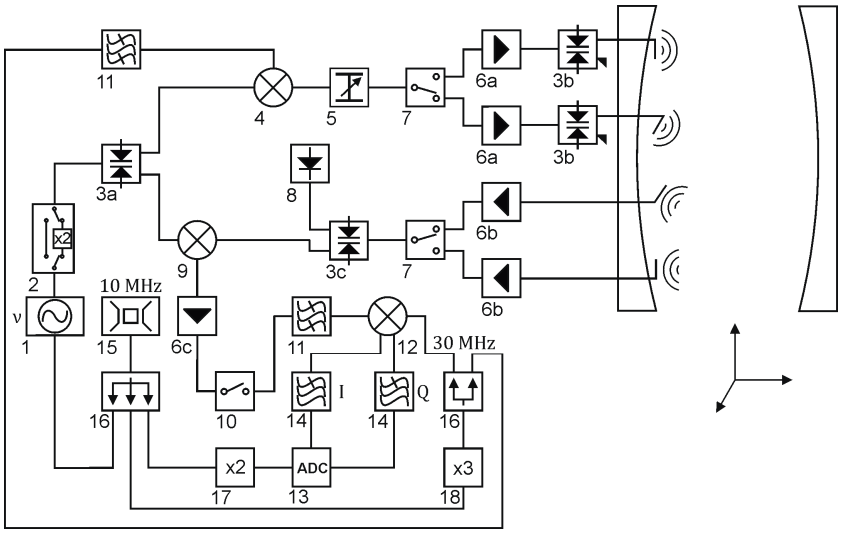

Fig. 5. The block scheme of the FTMW spectrometer; the components are described in the paper.

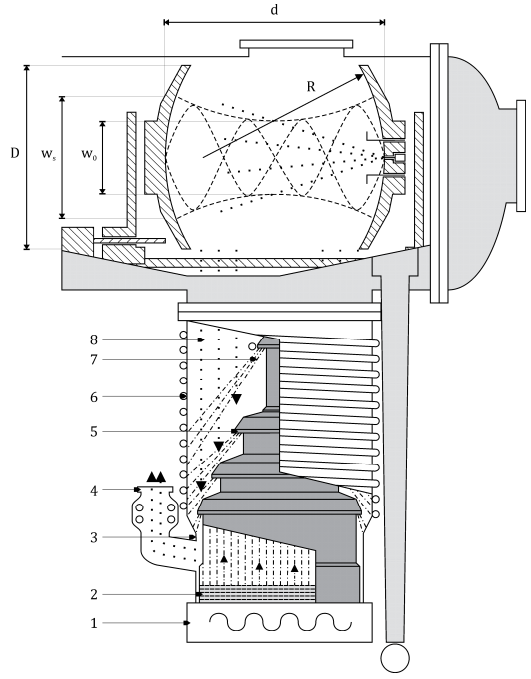

Fig. 6. Spectrometer arrangement with diffusion vacuum pump: (1) heater, (2) oil storage tank, (3) casing, (4) connection to the oil-sealed rotary vane pump, (5) nozzles, (6) cooling, (7) oil vapor jets and (8) evacuated molecules.

resonator does not exceed $5 \cdot 10^{-4}$ mbar even in case of 1 ms supersonic gas pulse duration and a pulse repetition frequency equal to 20 Hz. The block scheme of the overall system is shown in Fig. 5 and the spectrometer arrangement is shown in Fig. 6.

The primary harmonic signal f_0 is generated by the microwave generator (1) Rohde&Schwarz SMF100A operated within the frequency range of 1 - 22 GHz that is extended by the active frequency doubler Hittite HMC576LC3B and switches HMC547LC3 (2). The PIN diode single-pole-double-throw (SPDT) switch SIERRA MICROWAVE SFD0526 (3a) is employed to switch between the excitation and receiving part of the spectrometer. In the transmission mode, the monochromatic excitation microwave pulse is up-converted to the frequency f_0 + 30 MHz by the single side band (SSB) modulator MITEQ SM0226LC1MDA (4) with suppressed lower band. The second band and carrier suppression better than 20 dB is improved by the FP resonator selectivity. If the excitation pulse is not generated, the spectrometer is switched into the receiving mode, in which the synthesized signal is used to convert the detected response f_0 + 30 MHz + Δf, emitted by the measured gaseous sample, to the intermediate frequency 30 MHz + Δf.

The optimal polarization conditions depend on the matrix elements of the transition dipole moment of the molecular system, therefore the power of the excitation signal can be adjusted by the variable attenuator HMC939LP4E (5) and amplified by pairs of chip amplifiers HMC-ALH482 and HMC-ALH476 (6a), which also compensate for the conversion losses of the SSB modulator (4). The optimal frequency bands of the excitation signal can then be selected by Agilent 8765C electromechanical SPDT switches (7). The noise signal from the excitation part of the spectrometer, amplified by amplifiers (6a), is switched by SPDT switches (3b) to the load in the receiving mode. Only in the case of the transmission mode do these switches route the signal to the excitation antennas outputs. The maximal power delivered to the antennas depends mainly on the amplifier compression point (14 dBm), frequency dependent PIN diode switches, and antenna coupling element impedance.

The emission of the gaseous sample f_0 + 30 MHz + Δf is detected by the receiving antennas and amplified by the low-noise amplifier (6b) that is identical to (6a). In the case of the resonator tuning, the signal from the resonator is switched to the Schottky diode detector (8). Given the

transmission characteristics, the resonator is then tuned to the required resonant frequency.

The signal from the gas emission is down-converted by means of the MITEQ IRM0226LC1A image rejection mixer (IRM, 9) to the intermediate frequency of 30 MHz + Δf. The amplifier (6c) compensates for the conversion losses of the IRMs (9). In order to prevent the band-pass frequency filters from saturating (primarily from the decaying part of the excitation impulse), the protective switch (10) is used. The signal is subsequently filtered (11), converted to the base band by quadrature demodulator (12) and recorded (13) for analysis. The low-pass filters (14) remove other products and spurs from the quadrature mixer (12).

The overall spectrometer system utilizes the rubidium atomic clock (15) as a reference signal standard. Its long-term stability is improved by the i-Lotus M12M Timing Oncore Receiver with precise GPS timing. The reference signals are distributed by the distribution amplifier (16). The transient signal recorder (8 bit analog to the National Instruments NI PCI-5114 digital converter card), (13) employs the 20 MHz timing signal generated by the frequency doubler (17). For the SSB modulator (4) and quadrature mixer (12), the 30 MHz reference signal obtained from the frequency tripler (18) is used. The FTMW spectrometer is portrayed in Fig. 7.

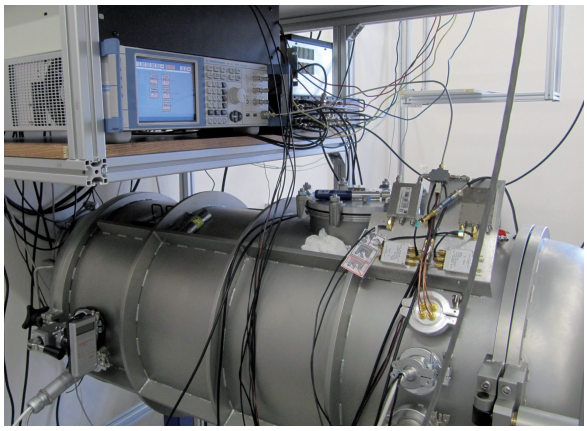

Fig. 7. Vacuum tank of Prague's FTMW spectrometer.

When the evacuation of the cavity is accomplished, the resonator is mechanically tuned up by adjusting the distance between the mirrors in order to achieve a resonant frequency that is equal to the frequency of excitation signal. This frequency should correspond to the centre frequency of the measured frequency band. Since the resonator is tuned up, the gas sample is injected into the FP cavity by means of the pulse solenoid valve and supersonic expansion jet. Therefore, the gas sample is cooled to approx. 90 K. In addition, as the jet is oriented parallel to the microwave beam excitation, the interaction time between the gas molecules and radiated pulse is extended, which leads to a high sensitivity of the measurement. On the contrary, Doppler effects split each spectral line into two components. This is caused by the gas molecules that are expanded in the resonator in one direction but emit electromagnetic radiation due to their polarization in both directions, thus generating a red and a blue shifted emission signal.

At the beginning of the gas expansion, the molecules are in thermodynamic equilibrium and the lower quantum state population is slightly smaller than in the upper state. From the macroscopic point of view, the gas molecules are randomly oriented as well. As the gas is expanding into the cavity, the rotational states are cooled. This results in a significant reduction of the excited states population. The molecules then interact with the microwave pulses within a time interval of about one to a few μs. Due to the on-off modulation of the excitation signal; the pulses are represented in the spectral domain by a narrow frequency band located around the resonant frequency (approx. 0.5 to 1 MHz). Frequencies corresponding to the frequencies of rotational states temporary cause absorption of the gas sample, its polarization and a nearly even distribution of both energy states. It means that after the interaction of microwave radiation, the molecules spontaneously emit energy. This emission typically lasts for from 100 to 500 μs. The final spectrum is thus obtained by converting the response into the frequency domain by means of the Fourier transform. The recorded signal is obtained at the central frequency equal to zero. As a result, the central frequencies of the spectra should be shifted from the zero frequency at the excitation frequencies.

4. Experimental Results

For the FTMW spectrometer developed, the molecule of the carbonyl sulfide $^{16}O^{12}C^{32}S$ was selected for obvious reasons as a suitable calibration molecule. First of all, this molecule is linear and hence its spectrum generally shows a low complexity. Furthermore, due to the zero nuclear magnetic moments of its constituents, there is no hyperfine structure to be resolved. It exhibits an appreciable dipole moment as well, so the spectral lines of transitions between the rotational quantum states exhibit an appreciable intensity in the spectrum. The fundamental rotational transition $J = 1 \leftarrow J = 0$ in the ground vibration state was measured. From the spectroscopic point of view, the fundamental transition is located at the frequency of approx. 12 GHz thanks to the relatively high molecular weight of $^{16}O^{12}C^{32}S$; see Fig. 8.

The use of a coaxially oriented beam and a FP resonator arrangement (COBRA) [12] in FTMW spectroscopy provides both high resolution and high sensitivity. To determine the sensitivity of our experimental arrangement measurements of the isotopically substituted OCS molecule were performed; see Fig. 9-11. The natural abundances of OCS isotopologues are as follows: $^{16}O^{12}C^{32}S$ 93.92 %, $^{16}O^{12}C^{34}S$ 4.15 %, $^{16}O^{13}C^{32}S$ 1.03 %, and $^{18}O^{12}C^{32}S$ 0.19 %. As for the resolution, the full widths at a half maximum (FWHM) of spectral lines are less than 10 kHz. An excep-

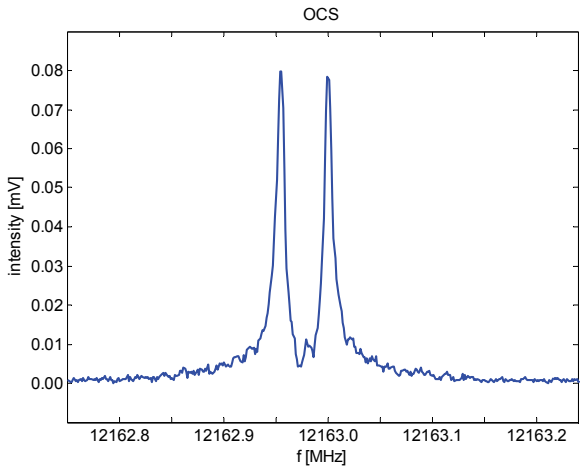

Fig. 8. The $J = 1 \leftarrow J = 0$ rotational transition of the $^{16}O^{12}C^{32}S$ measured using the supersonic molecular beam which is responsible for the Doppler doublet. The higher frequency component corresponds to the emission of the molecules approximating to the receiving antenna, the lower component is generated by the molecules moving away.

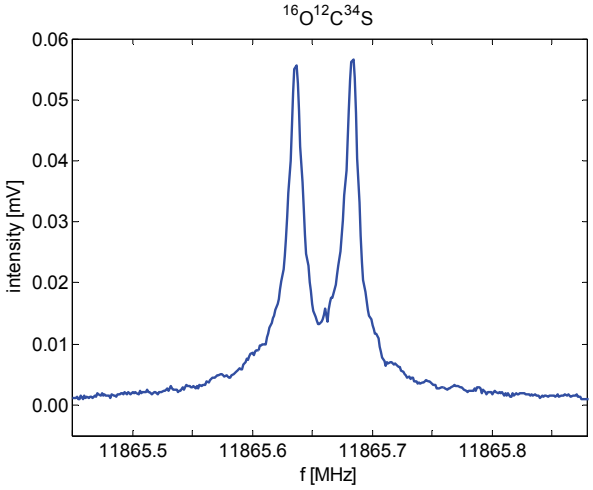

Fig. 9. The analogous Doppler doublet of the $^{16}O^{12}C^{34}S$ isotopologue whose natural abundance is more 20 times smaller (see text at Fig. 8).

tion can be observed for the $^{16}O^{13}C^{32}S$ isotopologue in Fig. 10. Due to the non-zero nuclear spin and to the corresponding magnetic moment of ^{13}C atom, there is a magnetic spin rotation hyperfine interaction which causes a significant line broadening. The observed FWHM is about twice as large as those for the other isotopologues.

As a result of the jet expansion being directed along the resonator axis, the Doppler doublet consisting of two frequency components appears in the spectra. The molecular resonance frequency is subsequently recovered as the arithmetic mean of the two Doppler components. The mean velocity of molecules could be evaluated from the frequency difference between the two components; for the presented spectra the mean velocity of the molecules is about 550 m/s. The bromomethane molecule is selected for the subsequent spectrometer testing; see Fig. 12.

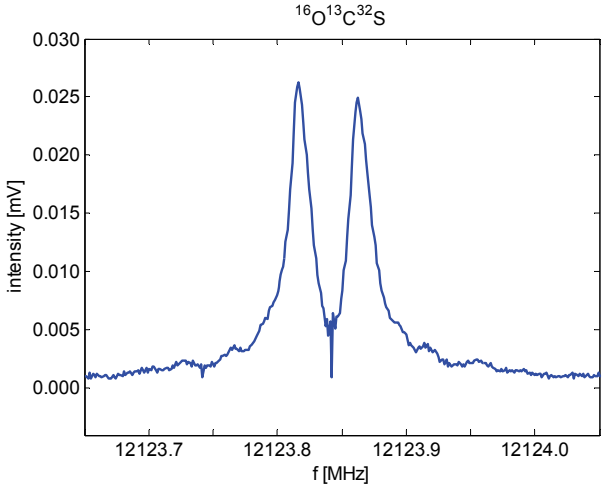

Fig. 10. The cognate Doppler doublet of the $^{16}O^{13}C^{32}S$ isotopologue whose abundance is 90 times smaller. The nucleus ^{13}C carries spin $I = 1/2$ and a magnetic moment. The corresponding magnetic interactions cause a significant line broadening.

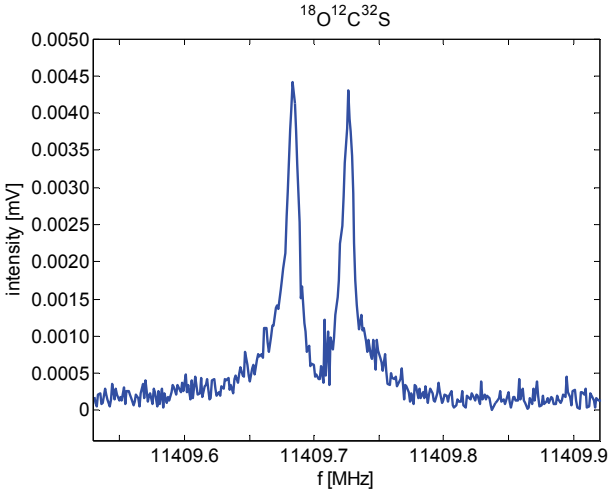

Fig. 11. The analogous Doppler doublet of the $^{18}O^{12}C^{32}S$ isotopologue whose concentration in a natural sample is nearly 500 times smaller than in the basic isotopologues.

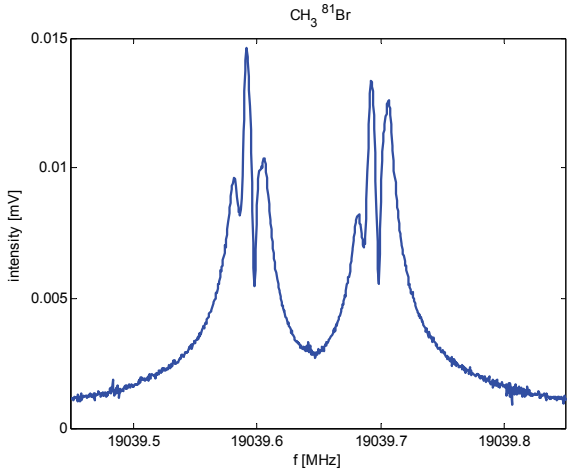

Fig. 12. The Doppler doublet of the $CH_3{}^{81}Br$ quadrupole hyperfine component 5/2←3/2 of the 1←0 rotational transition. The hydrogen magnetic hyperfine structure is partly resolved (triplet).

The presented spectrum shows the $CH_3{}^{81}Br$ 5/2←3/2 quadrupole hyperfine component of the rotational transition 1,0←0,0 (*J*,*K*). The quadrupole hyperfine structure is a consequence of the interaction between the electric quadrupole moment of the ^{81}Br nucleus (nuclear spin $I = 3/2$) with the intermolecular electric field gradient generated by the unsymmetrical distribution of charges within the molecule. The 5/2←3/2 quadrupole component is just one of the three possible quadrupole components within the rotational 1←0 transition. Besides the quadrupole splitting, there is another hyperfine structure that is a consequence of magnetic spin-rotational interactions between the hydrogen nuclear magnetic moments and the magnetic field generated by the rotation of the molecule [1,2]. While the 1,0←0,0 rotational spacing is about 19 GHz, the quadrupole spacing in the $|J = 1, K = 0\rangle$ level is about 150 MHz and the corresponding hydrogen magnetic splitting is only around 10 kHz (see Fig. 12). The magnetic hydrogen splitting of the rotational 1,0←0,0 transition in CH_3Br was observed for the first time.

The presented measurements show very good sensitivity of the spectrometer. The highest value of obtained voltage is approx. 0.08 mV, see Fig. 8. The maximal noise voltage is approx. 0.75 μV, see Fig. 12. The sensitivity is higher than 40 dB.

5. Conclusions

The design and construction of the Fourier Transform Microwave Spectrometer based on the Fabry-Perot resonator and the samples of measured spectra were presented. The frequency accuracy relies on the rubidium atomic clock and via GPS on cesium frequency standards. Above all, the presented spectra show very high frequency resolution. Furthermore, it is possible to observe the hyperfine structure in the spectra shape. In the case of low pressure of the measured sample, the amount of molecules is small; hence the power of emitted signal is very weak. The dynamics exceeding 40 dB promises a very high sensitivity of the spectrometer.

The FTMW spectrometer presented is a very useful tool for analyses of gaseous samples in the cm-wave frequency region for the following reasons: a wide range of Fabry-Perot resonator tunability, a wide frequency range and high sensitivity of the overall spectrometer system, high frequency resolution and precision. In addition to this, the extremely high spectral resolution, the emission arrangement, and the cm-wave frequency region make possible detailed studies of large organic molecules in the gaseous phase, such as pheromones, molecules of the human scent etc. that are not approachable by other experimental techniques. We believe this high resolution emission spectroscopy in the cm region also has great possibilities in diverse applications, such medical diagnostics, criminology identification of persons as well as in other areas where the molecular biology of gaseous samples can be utilized.

Acknowledgements

This research is a part of the joint activities of the Dept. of Electromagnetic Field of the Czech Technical University in Prague and the Dept. of Analytical Chemistry of the Institute of Chemical Technology. It gained financial support within the P206/10/2182 and P206/10/P481 research projects granted by the Czech Science Foundation and the Ministry of Education, Youth and Sports of the Czech Republic. In addition, it is financed also through the program C70 Development of Interdisciplinary Studies in Chemistry and Electrical Engineering and the specific university research program No. MSMT 21/2012.

References

[1] TOWNES, C. H., SCHAWLOW, A. L. *Microwave Spectroscopy.* London: McGraw-Hill, 1955.

[2] GORDY, W., COOK, R. L. *Microwave Molecular Spectra*. New York: Wiley, 1970.

[3] YAMADA, K. M. T. *Interstellar Molecules*. Heidelberg: Springer-Verlag, 2011.

[4] BALLE, T. J., CAMPBELL, E. J., KEENAN, M. R., FLYGARE, W. H. A new method for observing the rotational spectra of weak molecular complexes: KrHCl. *Journal of Chemical Physic*, 1979, vol. 71, no. 6, p. 2723 - 2725.

[5] BALLE, T., J., FLYGARE, W. H. Fabry-Perot cavity pulsed Fourier Transform Microwave Spectrometer with a pulsed nozzle particle source. *Review of Scientific Instruments*, 1981, vol. 52, no. 1, p. 33–45.

[6] SCOLES, G. *Atomic and Molecular Beam Methods*. New York: Oxford University Press, 1988.

[7] GRABOW, J.-U. Fourier Transform Microwave Spectroscopy measurement and instrumentation. *Handbook of High-resolution Spectroscopy*. John Wiley & Sons, Ltd, 2011, p. 723–799.

[8] ZVANOVEC, S., CERNY, P., PIKSA, P., KORINEK, T., PECHAC, P., et al. The use of the Fabry-Perot interferometer for high resolution microwave spectroscopy. *Journal of Molecular Spectroscopy*, 2009, vol. 256, no. 1, p. 141–145.

[9] KANIA, P., STUDECKY, T., CERNY, P., URBAN, T. Emission rotational spectroscopy of gases in the decimeter spectral region as a powerful tool for conformational analysis of complex molecules. *Chemicke Listy*, 2012, vol. 109, no. 10, p. 945–952. (in Czech)

[10] ZIMMERER, R. W. Spherical mirror Fabry-Perot resonators. *IEEE Transactions on Microwave Theory and Techniques*, Sep. 1963, vol. 11, no. 5, p. 371–379.

[11] FOX, A. G., LI, T. Resonant modes in a maser interferometer. *Bell System Technical Journal*, Mar. 1961, vol. 40, p. 453–488.

[12] GRABOW, J.-U., STAHL, W., DREIZLER, H. A multioctave coaxially oriented beam-resonator arrangement Fourier-transform microwave spectrometer. *Review of Scientific Instruments,* 1996, vol. 67, no. 12, p. 4072–4084.

About Authors ...

Václav KABOUREK was born in 1985. He received his M.Sc. degree from the Czech Technical University in Pra-

gue in 2010. His research interests include UWB communication, RCS measurement, microwave detection of non-metallic object, analysis and development of detection techniques and signal transformations in MATLAB.

Petr ČERNÝ was born in 1976. He was awarded his M.Sc. and Ph.D. degrees by the Czech Technical University in Prague in 2001 and 2008, respectively. His contemporary research activities are focused on high-resolution microwave and terahertz spectroscopy, microwave circuits and antennas, ultra wideband devices and die bonding. He is a member of the IEEE and the Radioengineering Society.

Petr PIKSA was born in 1977. He received his M.Sc. degree in 2002 and Ph.D. degree in 2007 from the Czech Technical University in Prague. His interests are in the field of planar antennas, modeling of electromagnetic fields, quasi-optics, millimeter wave measurements and microwave spectroscopy measurements. He is a member of the Radioengineering Society.

Tomáš STUDECKÝ was born in 1986. He received the M.Sc. degree after graduating from the Institute of Chemical Technology in Prague in 2012. He is currently a Ph.D. student at the Department of Analytical Chemistry. His contemporary research activities are focused on Fourier Transform Microwave Spectroscopy.

Patrik KANIA was born in 1977. He received the M.Sc. and Ph.D. degrees in Analytical Chemistry from the Institute of Chemical Technology Prague in 2001 and 2006, respectively. His research interests include the high resolution rotational spectroscopy of atmospherically and astrophysically important molecules and the design of millimeter wave spectrometers.

Štěpán URBAN was born in 1950 in Prague. He received his M.Sc. in Physical Chemistry from Charles University in Prague and the Ph.D. degree in Chemical Physics from the Czechoslovak Academy of Sciences. In 2004, he was appointed to a full professorship at the Institute of Chemical Technology, where he was named as the head of the Department of Analytical Chemistry in 2008. Since 2006, he is the 1st vice-president of the Ioannes Marcus Marci Spectroscopic Society. He is a member of the J. Mol. Spectroscopy editorial board and the chairman of the biennial International Conferences on the High-Resolution Spectroscopy. Both theoretical and experimental high resolution spectroscopies are subjects of his research interest.